Nanoscale

Accepted Manuscript

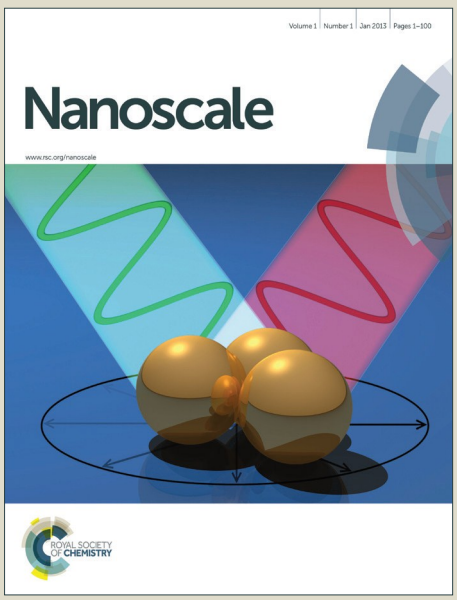

This is an *Accepted Manuscript*, which has been through the Royal Society of Chemistry peer review process and has been accepted for publication.

Accepted Manuscripts are published online shortly after acceptance, before technical editing, formatting and proof reading. Using this free service, authors can make their results available to the community, in citable form, before we publish the edited article. We will replace this *Accepted Manuscript* with the edited and formatted *Advance Article* as soon as it is available.

You can find more information about *Accepted Manuscripts* in the Information for Authors.

Please note that technical editing may introduce minor changes to the text and/or graphics, which may alter content. The journal's standard Terms & Conditions and the Ethical guidelines still apply. In no event shall the Royal Society of Chemistry be held responsible for any errors or omissions in this *Accepted Manuscript* or any consequences arising from the use of any information it contains.

ROYAL SOCIETY OF CHEMISTRY

www.rsc.org/nanoscale

Hydrogen bonding vs molecule-surface interactions in 2D self-assembly of [C60]fullerenecarboxylic acids

Mohamed A. Mezour, Rachelle M. Choueiri, Olena Lukoyanova, R. Bruce Lennox[*]*, Dmitrii F. Perepichka* [*]

Department of Chemistry and Centre for Self-Assembled Chemical Structures, McGill University, 801 Sherbrooke St. West, Montreal (QC) H3A 0B8, Canada

ABSTRACT

The adsorption of C_{60}-malonic derivatives $C_{61}(CO_2H)_2$ and $C_{66}(CO_2H)_{12}$ on Au(111) and a pentaflurobenzenethiol-modified Au substrate (PFBT-Au) has been investigated using scanning tunneling microscopy (STM) at a liquid-solid interface. Monofunctionalized $C_{61}(CO_2H)_2$ forms a hexagonal close-packed overlayer on Au(111) and individual aligned dimers on PFBT@Au(111). The difference is attributed to the nature of substrate…$C_{61}(CO_2H)_2$ interaction (isotropic π-Au bonding vs anisotropic PFBT...COOH interactions). Surprisingly, in both cases, the directionality of COOH…COOH motif is compromised in favor of synergistic van der Waals/H bonding interactions. Such van der Waals contacts are geometrically unfeasible in hexafunctionalized $C_{66}(CO_2H)_{12}$ and its assembly on Au(111) leads to a 2D molecular network controlled exclusively by H bonding. For both molecules, the "free" CO_2H groups on monolayers surface can engage in out-of-plane H bonding interaction resulting in an epitaxial growth of subsequent molecular layers.

TOC

Pentafluorobenzenethiol SAM stabilizes fullerenecarboxylic acids at a solid-liquid interface enabling their STM imaging as individual clusters at room temperature

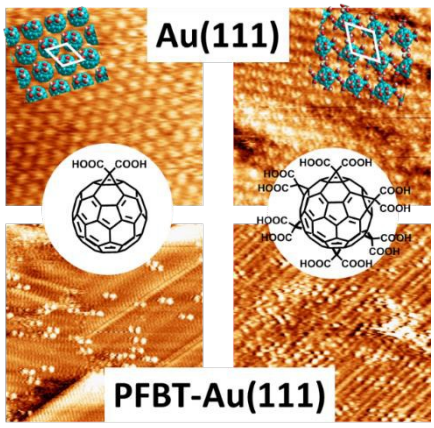

Nanoscale Accepted Manuscript

INTRODUCTION

Due to their unique electronic, magnetic and chemical properties, fullerenes and their derivatives have been extensively explored for a variety of applications, notably organic photovoltaic cells,[1,2] field effect transistors,[3,4,5] and superconductors.[6,7,8] The charge-transport characteristics and overall performance of the C_{60}-based devices relies largely on the morphological order of the C_{60} component, in bulk and at the interface.[9,10] Thus, various chemical and physical methods have been used to control the arrangement and pattern C_{60} on surfaces.[11]

In this context, supramolecular self-assembly provides a means to create complex structures and patterns of C_{60} molecules with sub-nanometer precision over an extended length scale.[12] Such structures are governed by a subtle interplay of intermolecular and molecule-substrate interactions.[13] When deposited on metal surfaces, C_{60} itself self-assembles into hexagonal close packed (hcp) layers.[14,15,16] More complex fullerene architectures can be created by pre-patterning the substrate with a molecular template that accommodates individual C_{60} molecules, either through the host-guest interactions within a porous network (oligothiophene,[17,18] trimesic acids,[19] calix[8]arene,[20] perylenediimide-melamine[21]) or through donor-acceptor interactions on top of self-assembled molecular networks of electron rich molecules (porphyrin,[22] α-sexithiophene,[23] coronene[24], and pentacene[25]). In these cases, the assembly is dominated by molecule-substrate interactions rather than weaker van der Waals (vdW) C_{60}...C_{60} interations. On the other hand, strengthening intermolecular interactions via H bonds offers a higher level of control over the molecular self-assembly process and provides a way toward programmable supramolecular structures for potential applications in optoelectronic devices.[26,27]

H bonding has been widely exploited in solution-based chemistry to direct the assembly of C_{60} molecules. This includes highly stable fullerene dimers prepared through self-complementary H bonding motifs,[28,29] C_{60}–donor complexes (e.g., with porphyrin donor),[30,31] and H bonded C_{60} supramolecular polymers.[32] In contrast, the 2D H bonded C60 assemblies were rarely investigated.[33] Zhou et al reported a self-ordered monolayers of fullerene derivatives assembled via self-complementary trident H bonding.[34] The only other study of H bonded fullerene on a surface is ultra-high vacuum STM of C_{60}-functionalized malonic acid ($C_{61}(CO_2H)_2$) adlayer on Au(111), which revealed the formation of a hexagonal close packed structure.[35]

In this work, we explore the effect of intermolecular and molecule-substrate interactions on self-assembly of fullerene derivatives functionalized with H bonded groups. Specifically, we investigate the assembly of multicarboxylic acid derivatives of C_{60} ($C_{61}(CO_2H)_2$ and $C_{66}(CO_2H)_{12}$) on bare Au(111) and

Nanoscale Accepted Manuscript

a pentafluorobenzenethiol (PFBT) modified Au(111) substrates at liquid-solid interface. Periodic 2D assemblies (hexagonal, oblique) are formed on bare Au(111), while only isolated stable clusters, oriented along the $\langle 1\bar{1}0 \rangle$ direction of Au (111), were observed on PFBT self-assembled monolayer (SAM) substrate. This study emphasizes the important role of the SAM in controlling the structure of organic semiconducting materials at the interface.

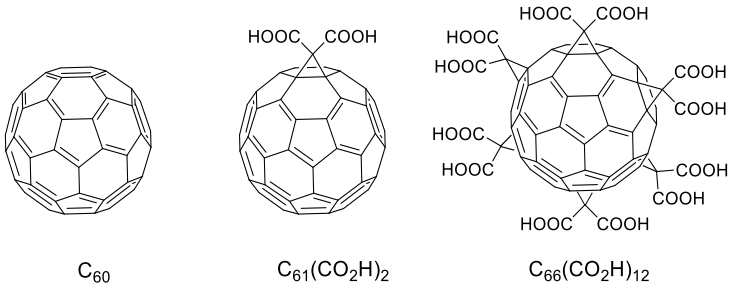

RESULTS AND DISCUSSION

$C_{61}(CO_2H)_2$ assembly on Au(111)

Fig. 1 shows a representative STM image of $C_{61}(CO_2H)_2$ adlayer obtained at a liquid-solid interface after drop casting a saturated phenyloctane solution of $C_{61}(CO_2H)_2$ onto Au(111). The individual molecules appear as featureless bright spots with a diameter of ca. 0.7 nm. This assignment is supported by the size of vacancies and admolecules in the monolayer, showing as dark and bright spots, respectively (highlighted by circles in Fig. 1b).

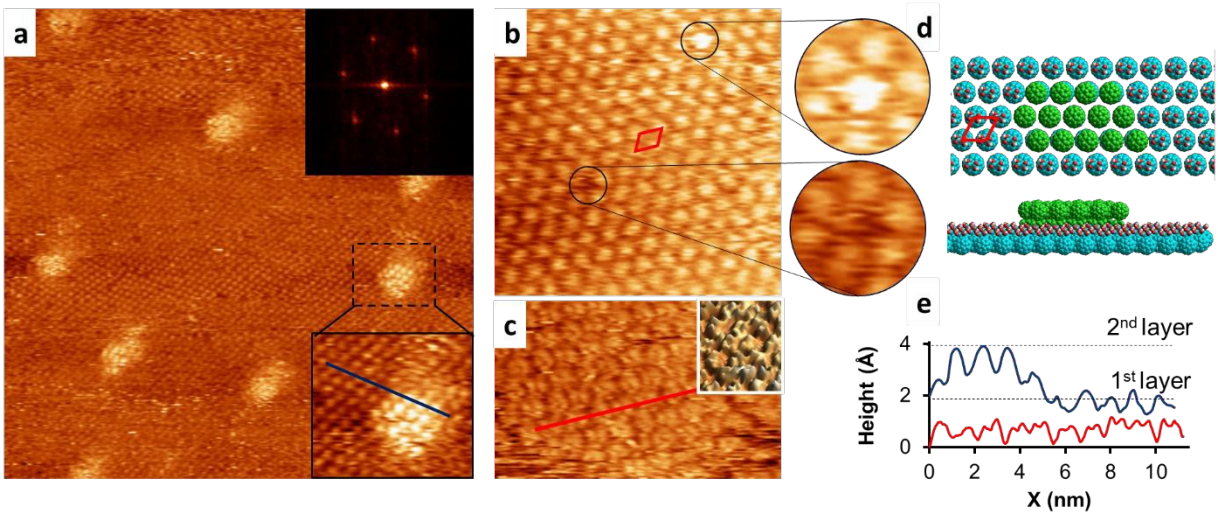

Fig. 1. STM of a $C_{61}(CO_2H)_2$ monolayer at phenyloctane/Au (111) interface: (a) a representative 76 × 76 nm^2 micrograph, 2D FFT of the image (top inset) and 15 × 15 nm^2 close-up on the second molecular layer (bottom inset); (b) 21 × 21 nm micrograph showing the unit cell; the circles highlight a missing and an ad-molecule in the monolayer; (c) 14 × 7 nm^2 micrograph showing a submolecular resolution with

Nanoscale Accepted Manuscript

corresponding 3D view in inset; (d) molecular model (top and side view) showing two hcp layers of $C_{61}(CO_2H)_2$; (e) cross section profile along the blue and red lines in (a and c). V_b = 600 mV, I_t = 0.2 nA (a,b); V_b = 800 mV, I_t = 0.3 nA (c).

The high resolution STM image (Fig. 1b) and a 2D Fast Fourier Transform (FFT, inset in Fig. 1a) reveal a hexagonal close packed arrangement of $C_{61}(CO_2H)_2$ with unit cell parameters of $a = b = 1.0 \pm 0.1$ nm, $\alpha = 60 \pm 3°$, assigned to $(2\sqrt{3} \times 2\sqrt{3})R30°$ overlayer structure on Au(111). This is consistent with previous UHV STM study of $C_{61}(CO_2H)_2$.[35] Similar molecular packing has also been reported for non-functionalized C_{60} adsorbed on Au(111) in ambient,[36] UHV[37,38] conditions, and observed for C_{60} (Fig. S1) at a liquid-solid interface[39].

At certain tunnelling conditions, higher brightness features have been resolved on top of $C_{61}(CO_2H)_2$ (Fig. 1c,e). These features could likely be attributed to CO_2H groups, as previously suggested in ultra-high vacuum STM studies of this molecule.[35] It was earlier suggested[35] that the observed hcp assembly of C_{61}-$(CO_2H)_2$ is driven by a network of strong $R^3_3(9)$[40] H bonds between *all* CO_2H groups of adjacent molecules. However, the DFT modeling (Fig. 2) shows that in the observed close-packed structure, only one of the CO_2H groups can engage in H bonding interactions with the neighboring molecules, either via $R^2_2(8)$ dimers or $R^3_3(12)$ trimers, above the molecular 2D crystal plane (Fig. 2). Both M06-2X and B3LYP (with empirical dispersion correction GD3BJ, see SI) functional calculations suggest that H bonding in $C_{61}(CO_2H)_2$ can act cooperatively with π-π (van der Waals) interactions. The latter can be estimated to account for ca. 20 kcal/mol in a hexagonally packed C60 monolayer (ca. ½ of the experimental ΔH_{sub} = 40-44 kcal/mol[41]). An additional stabilization of ca. ~10 kcal/mol is afforded by either $R^2_2(8)$ (Dimer I) or $R^3_3(12)$ (Trimer) H bonding (Fig. 2 and Table S1).[18] Thus, at room temperature both H bonding motifs are expected to co-exist and dynamically interconvert, within the densely packed monolayer of $C_{61}(CO_2H)_2$ on Au(111).

Nanoscale Accepted Manuscript

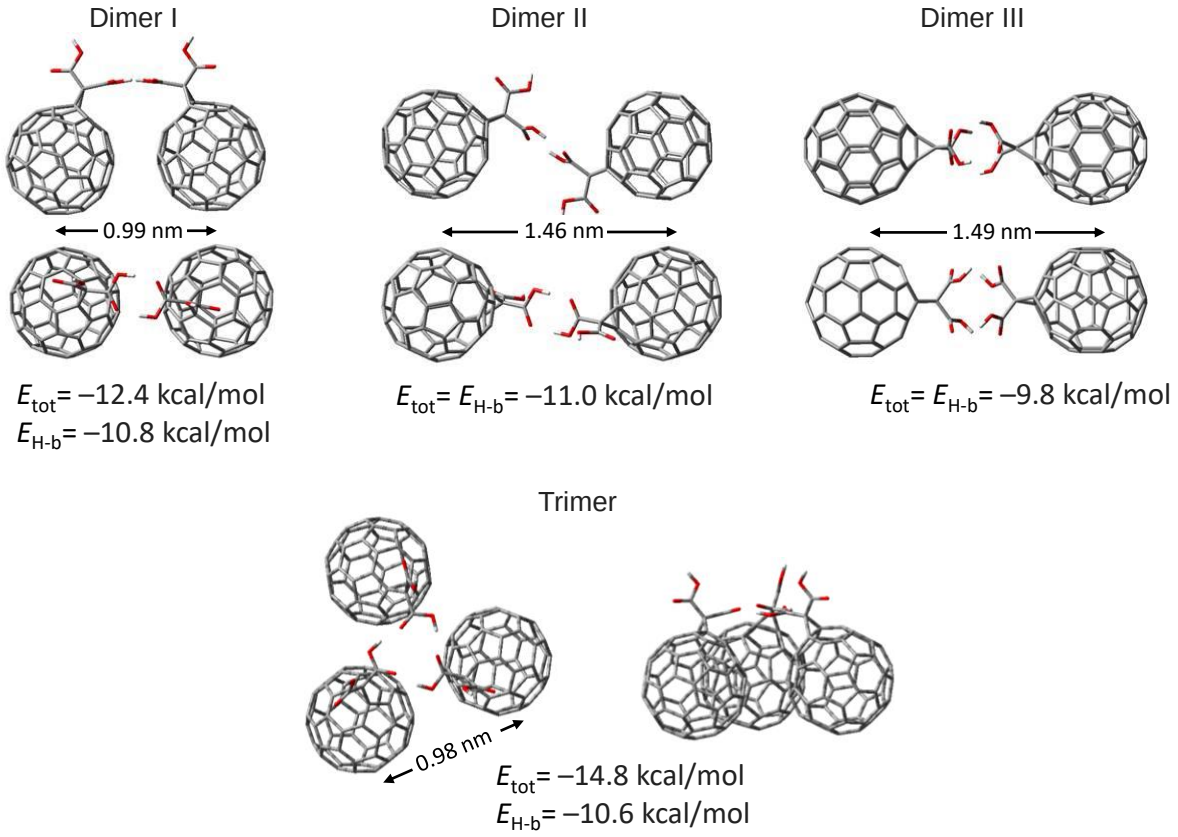

Fig. 2. DFT calculated (M06-2X/6-31G(d)) structures of possible H bonding dimers and trimer of $C_{61}(COOH)_2$ in gas phase (top and side views). E_{tot}: total binding energy, E_{H-b}: H bonding energy per molecule.

It is noteworthy, that the free COOH groups of a $C_{61}(CO_2H)_2$ adlayer are available to form H bonds with molecules of a second layer which probably explains the presence of small bright islands of $C_{61}(CO_2H)_2$ perfectly aligned with first molecular layer (Fig. 1a).

Overall, these arguments suggest that the $C_{61}(CO_2H)_2$ assembly is controlled primarily by strong molecule-substrate bonding and van der Waals (π–π) interactions between the fullerene cores. The H bonding above the adlayer plan could bring additional stabilization, but does not change the molecular packing. Indeed, a rather strong Au...C_{60} bonding was estimated both experimentally using temperature programmed desorption (TPD)[42] (~44 kcal/mol) and by DFT calculations (~35 kcal/mol).[43] The nature of this interaction has been the subject of numerous studies including high resolution angle resolved photoemission, NEXAFS, STM, and DFT calculations.[42,43,44,45] A covalent like character for the C_{60}-metal bonding was suggested from the observed hybridization between the d-states of the metal surface and the

Nanoscale Accepted Manuscript

π-orbitals at the C_{60} cage,[44] the significant charge transfer from the substrate to C_{60} (0.8 e^- per molecule[42]), and the surface reconstruction upon fullerene adsorption.[45]

$C_{61}(CO_2H)_2$ assembly on PFBT SAMs

In order to stir the self-assembly towards H bonding control, the molecule...surface interactions should be weakened; this can be achieved by modified the Au(111) surface with SAMs. However, the absorption energy of small molecules on typical SAMs is so low that the molecular self-assembly is generally not observed at a SAM-liquid interface. Recently, we have found an accelerated kinetics of adsorption of unfunctionalized C_{60} on PFBT, as compared to benzenethiol (BT) and octanethiol, and have decided to use it as a template for H bonded self-assembly.[46] SAM of PFBT on Au(111) is characterized by rows of molecules oriented along $\langle 1\bar{1}0 \rangle$ direction of the gold substrate, forming a $(2 \times 2\sqrt{3})$ 2D crystal lattice with two standing up molecules per unit cell.[46,47] In contrast to Au(111) surface, adsorption of $C_{61}(CO_2H)_2$ onto a PFBT-Au substrate at the solid-liquid interface did not yield a close-packed structure. Instead, a range of small $C_{61}(CO_2H)_2$ clusters were observed on the surface (Fig. 3).[48]

Nanoscale Accepted Manuscript

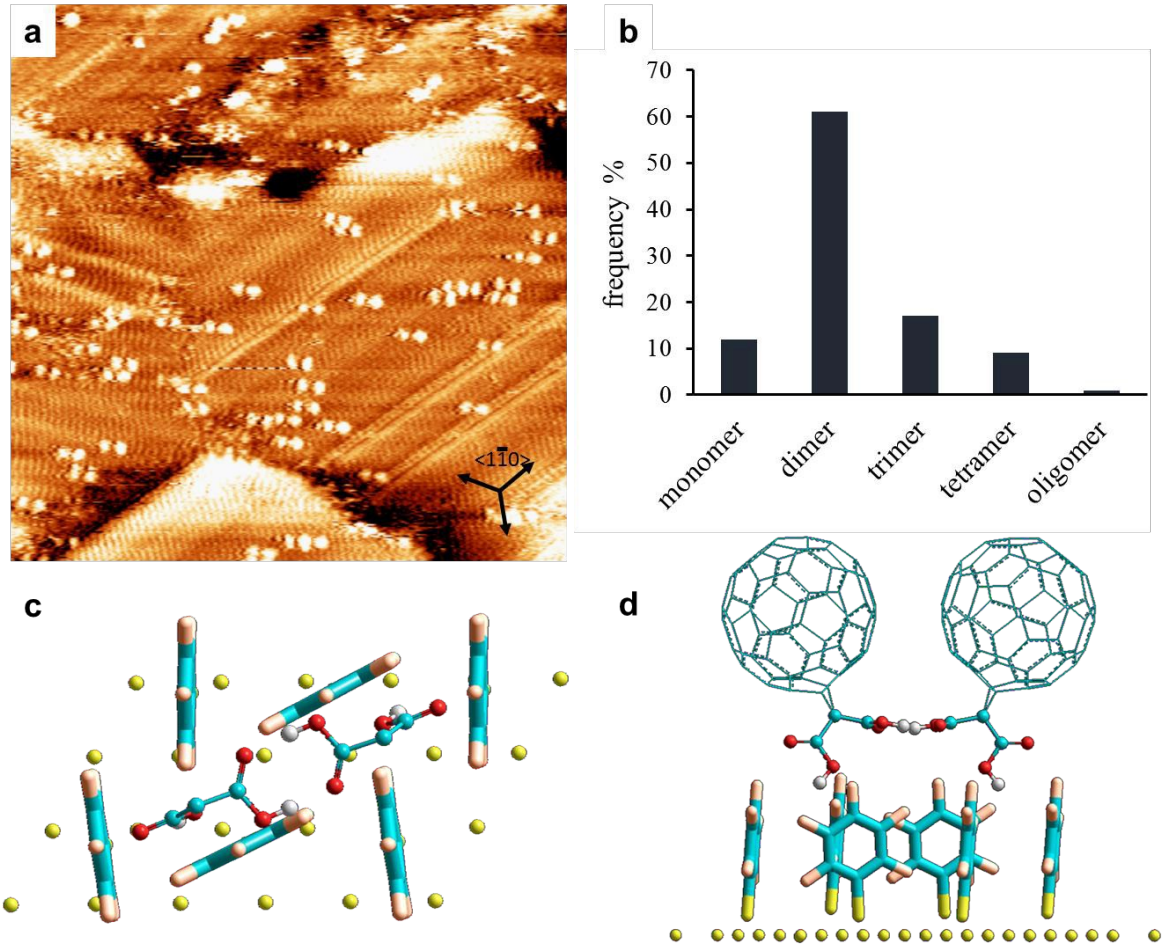

Fig. 3. (a) Representative 40 × 40 nm^2 STM image of $C_{61}(CO_2H)_2$ monolayer at phenyloctane/ PFBT@Au(111). (b) Histogram of $C_{61}(CO_2H)_2$ clusters distribution. (c),(d) Top and side view of the schematic presentation of C_{61}-$(CO_2H)_2$ dimers on top of PFBT SAM showing the inetrcalation of COOH groups between PFBT (for simplification, C60 are not presented in (c)).

Analysis of STM images (Fig. 3b) reveals the predominance of dimeric clusters (60%). Among the different possible structures of dimers, DFT suggests the greatest stability for dimer I in which the molecules encounter both the H bonding and vdW interactions (Fig. 2). Analysis of the molecular separation in these dimers shows a distance of $d_{1,2}$ = 1.0 ± 0.1 nm which is consistent with the molecular model of dimer I (0.99 nm). A control experiment with a fullerene malonic ester (C_{61}-$(CO_2Et)_2$) shows only randomly distributed individual molecules, confirming the critical role of the H bonding in the observed assembly (Fig. S3).

The observed H bonded dimers are remarkably immobile: very little drift in their location (~0.05 nm/s) was observed during STM scanning (Fig. S2). The low mobility reflects a large diffusion barrier at the SAM surface and we hypothesize this to be caused by interactions of the non-H bonded carboxylic

Nanoscale Accepted Manuscript

group of the fullerene and the pentrafluorophenyl ring of the SAM, which is estimated at ~6 kcal/mol from the gas phase calculations ($CH_3COOH…F_5C_6SH$, M06-2X/6-31G(d)).

Strong specific interactions with the surface are also implied by the preferential alignment of dimers along the $\langle 1\bar{1}0 \rangle$ direction of Au (111). This alignment does not seem to be induced by the scanning tip, since it is maintained upon the change of the scan direction (Fig. S2d,e). The specific nature of the COOH…PhF_5 interactions and intercalation of the protruding COOH group in the herringbone PFBT SAM (Fig. 3c,d) are likely responsible for the observed alignment. Both the immobilization and the preferential alignment suggest substantial corrugation and anisotropy in PFBT-covered surface.

The observed preference for dimers vs larger clusters is also readily explained by the specific interaction of PFBT layer with COOH groups of $C_{61}(CO_2H)_2$, which makes them "unavailable" for further H-bonding required for assembly or larger clusters.

$C_{66}(CO_2H)_{12}$ assembly

As a bidentate H bonding building block (two $R^2_2(8)$ synthons), $C_{61}(CO_2H)_2$ can only assemble into 1D chains. In order to create 2D networks using H bonding we employed $C_{66}(CO_2H)_{12}$ molecule with six malonic acid moieties aligned in the three orthogonal directions.[49] Adsorption of $C_{66}(CO_2H)_{12}$ onto Au(111) from a saturated phenyloctane solution results in the spontaneous formation of a 2D molecular structure with a typical domain size ca. 20–60 nm (Fig. 4a). A zoom-in of these domains reveals two bright protrusions on top of each molecule (Fig. 4b), as was observed for $C_{61}(CO_2H)_2$ and attributed to CO_2H groups. The assembly of $C_{66}(CO_2H)_{12}$ is characterized by an oblique unit cell that contains one molecule, which is distinctly different from the hcp arrangement of $C_{61}(CO_2H)_2$.

DFT optimized molecular model (M06-2X/6-31G(d) in periodic boundary conditions, PBC) predicts a unit cell similar to the experimental results (Fig. 4c). Each molecule is connected to its two neighbors through strong (type II, Fig. 2) H bonding of its two COOH groups, along *b* direction of the unit cell. The formed supramolecular chains are held together by weaker, geometrically distorted H bond (type III, Fig. 2) contacts of four other CO_2H groups along *a* direction. The model also shows that two other CO_2H groups in the *ab* plane are precluded from H bonding by the geometry of the network. Of the remaining four CO_2H groups (above and below *ab* plane), two are pointed towards Au(111) thus defining the molecule-surface interaction. The CO_2H-Au interaction has been previously reported for the standing up phase of trimesic acid (TMA) on Au(111).[50] Finally, the last two CO_2H groups are pointing away from the substrate enabling a potential bonding of a second layer. Indeed, a prolonged (18 h) immersion of Au substrate in $C_{66}(CO_2H)_{12}$ solution leads to the growth of a second layer (Fig. 5). Close inspection of the

Nanoscale Accepted Manuscript

$C_{66}(CO_2H)_{12}$ two layers shows a co-alignment of their unit cells suggesting their epitaxial relationship driven by the H-bonding.

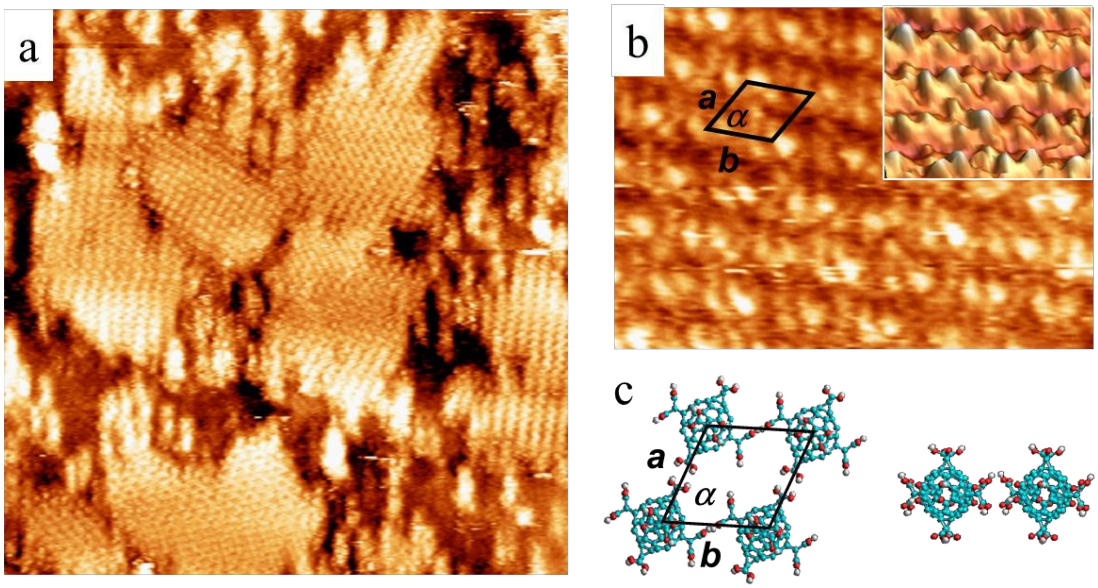

Fig. 4. (a) Representative 80 × 80 nm^2 STM images showing domains of a $C_{66}(CO_2H)_{12}$ at phenyloctane/Au (111) interface. (b) High resolution 10 × 10 nm^2 STM image showing the oblique unit cell (a=1.67±0.15 nm, b=1.55±0.15 nm α=69±4°); inset: 3D view of the 6 × 6 nm^2 STM image highlighting the submolecular features atop of the fullerene molecules. (c) DFT optimized model (top and side view) for 2D assembly of $C_{66}(CO_2H)_{12}$ (PBC); unit cell: a= 1.52 nm, b=1.47nm, α=66°. V_b = 800 mV, I_t = 0.15 nA.

Nanoscale Accepted Manuscript

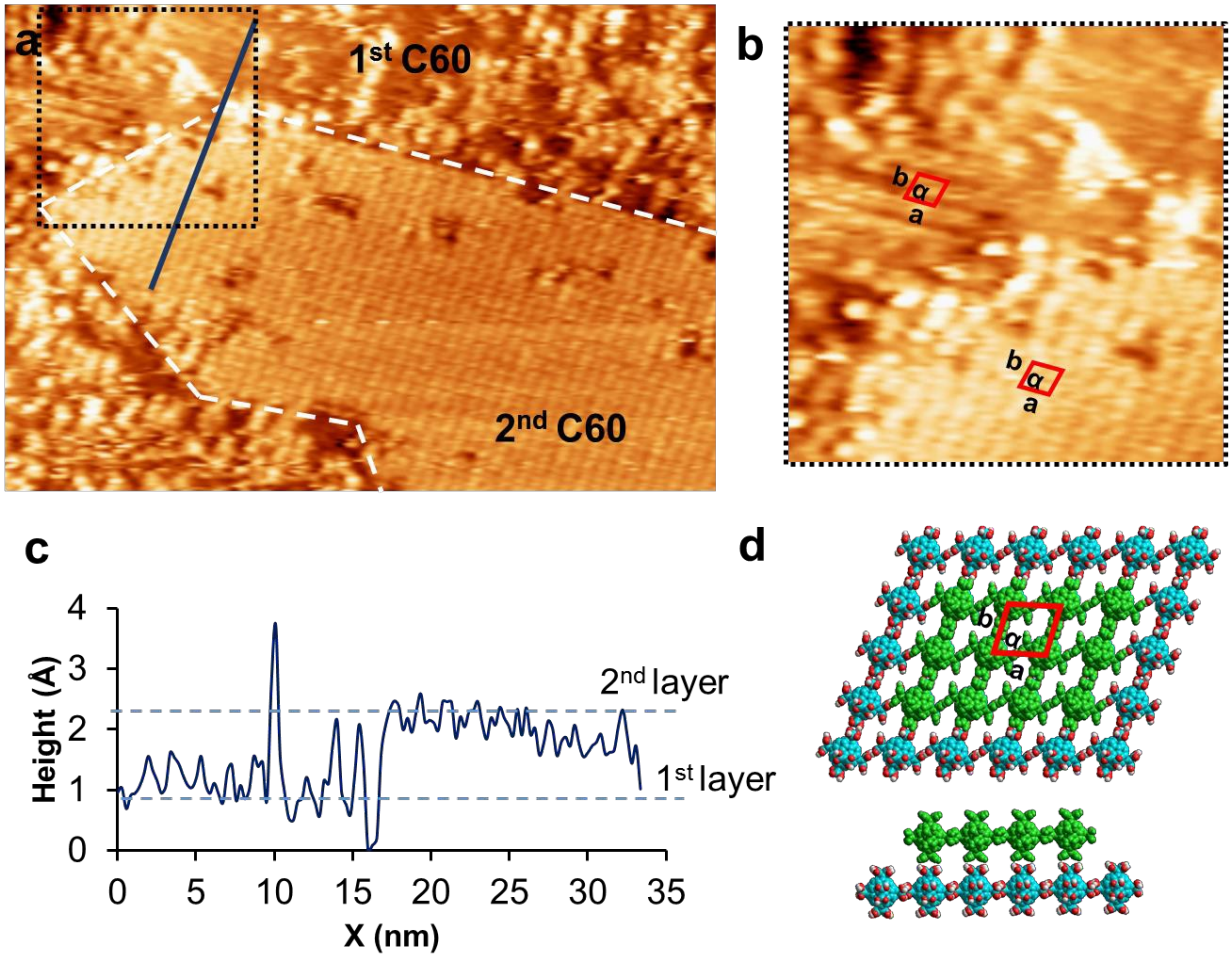

Fig. 5. (a) STM image showing two layers of $C_{66}(CO_2H)_{12}$ molecules at phenyloctane/Au (111) interface (90 × 57 nm^2). (b) Zoom in of the dashed square in (a) showing the coalignement of the unit cell in the first and second layers of $C_{66}(CO_2H)_{12}$ assembly. (c) Cross sectional profile along the blue line in (a). (d) Molecular model (Top and side view) of $C_{66}(CO_2H)_{12}$ bilayer. Unit cell. a=b=1.5± 0.1nm, α=68 ± 8°..V_b = 1000 mV, I_t = 0.15 nA.

Similar to $C_{61}(CO_2H)_2$, adsorption of $C_{66}(CO_2H)_{12}$ from phenyloctane on PFBT SAM@Au(111) substrate only gives rise to separate clusters, dominated by linear arrays of molecules that are aligned on top of PFBT (Fig. S4b). The spacing of the fullerene molecules in these clusters (~1.5 nm) corresponds to the periodicity of the $R^2_2(8)$ H bonding along **b** direction in the $C_{66}(CO_2H)_{12}$ 2D monolayer on Au(111). The protruding malonic acid moieties do not allow for π-π contacts of the fullerene core, as observed for $C_{61}(CO_2H)_2$ which showed a shorter intermolecular distance on PFBT (dimer I). The inability of $C_{66}(CO_2H)_{12}$ to form continuous 2D monolayer at liquid/PFBT SAM interface might be due to directional interactions of the free CO_2H group with the surface which destabilizes the interface of crystallographically non-commensurate layers (PFBT and $C_{66}(CO_2H)_{12}$).

Nanoscale Accepted Manuscript

CONCLUSIONS

The directionality, selectivity and relatively high strength of intermolecular H bonding have been exploited for the formation of mono and bilayers of [C_{60}]fullerene multicarboxylic acids derivatives (C_{61}-$(CO_2H)_2$ and $C_{66}(CO_2H)_{12}$). The resulting monolayer structure depends on the number and position of carboxylic functionalities. A hexagonal close packed monolayer structure of $C_{61}(CO_2H)_2$ on Au(111) is driven by the strong π-Au bonding (35–45 kcal/mol) and intermolecular vdW interactions (~20 kcal/mol). In contrast, in $C_{66}(CO_2H)_{12}$ the six malonic acid moieties oriented in three different directions sterically screen the π-surface and this compound forms an oblique H bonded molecular network via H bonding interactions. The free CO_2H groups on the surface of both monolayers act as cues inducing the growth of a subsequent layer(s), in an epitaxial relationship with the first monolayer. A chemisorbed SAM (PFBT) was shown to act as a 2D template controlling a supramolecular assembly of physisorbed molecules. The immobilization and alignment of *individual* C_{61}-$(CO_2H)_2$ dimers on top of PFBT SAM is most unusual for molecular assembly at room temperature, and was attributed to specific interactions of the stacked PFBT in its SAM, with 'free' COOH groups of physisorbed fullerene derivatives. We believe that expanding this approach to other chemisorbed/phisisorbed systems will provide new venues for bottom-up fabrication of complex functional nanostructures following the principles of molecular self-assembly.

EXPERIMENTAL SECTION

Fullerene derivatives $C_{61}(CO_2Et)_2$, $C_{61}(CO_2H)_2$, and $C_{66}(CO_2H)_{12}$ were prepared according to literature.[51,52,53]

Au(111) substrates with atomically flat terraces were prepared by thermal evaporation of gold onto freshly cleaved mica sheets preheated at 450 °C under a pressure of 10^{-7}-10^{-8} Pa. The SAMs of pentafluorobenzenethiol (PFBT) were prepared by immersing the Au/mica in a 0.1 mM EtOH (ACS reagent) solution of the corresponding thiols at 60 °C for 2 to 18 hours. After SAM formation, the samples were rinsed with pure EtOH and dried under a stream of ultrapure N_2. A drop (10–15 μL) of saturated phenyloctane solutions of C_{60} derivatives has been deposited on bare Au(111) or on PFBT-Au substrate and the resulting assembly has been imaged immediately, at a liquid–solid interface.

All STM experiments were performed using Multimode 8™ equipped with a Nanoscope™ V controller (Bruker, Santa Barbara, CA) and Nanoscope 8.15r3 software. The STM tips were mechanically cut from Pt/Ir wire (80/20, diameter 0.25 mm, Nanoscience). All STM-images were obtained in the

Nanoscale Accepted Manuscript

constant current mode using an A scanner and low current STM converter. Calibration of the piezoelectric positioners was verified by atomic resolution imaging of graphite. The raw images were processed from WSxM5.0 software.

All density functional theory (DFT) calculations were carried out using the Gaussian 09 program package. Geometry optimization have been performed using the M06-2X and the B3LYP functional with the polarized 6-31G(d) basis set. The Becke–Johnson damping (GD3BJ) has been used in B3LYP calculations to account for the empirical dispersion effect. For $C_{61}(CO_2H)_2$, the optimized conformation of the monomer, three configurations of dimers and the trimer have been determined. Hydrogen bonding energy per molecule in these cluster were computed by subtracting the energy π-π interactions between fullerene core (estimated from the energy of the same cluster structure of C_{60} molecules without malonic acid group) from the total binding energy. DFT calculation of $C_{66}(CO_2H)_{12}$ was performed with periodic boundary conditions (PBC).

Supporting Information. Supporting Information is available from the Wiley Online Library or from the author: STM of C_{60} on Au(111), additional STMs for $C_{61}(CO_2H)_2$, $C_{61}(CO_2Et)_2$ and $C_{66}(CO_2H)_{12}$ on PFBT and BT modified Au(111). Tabulated results of DFT calculations.

Corresponding Author
Bruce.Lennox@mcgill.ca; Dmitrii.Perepichka@mcgill.ca.

ACKNOWLEDGMENT
This work was supported by NSERC-Discovery and FQRNT-Team Grants. M.A.M. thanks NSERC and FQRNT for doctoral fellowships.

Nanoscale Accepted Manuscript

REFERENCES

1 G. Yu, J. Gao, J. C. Hummelen, F. Wudl and A. J. Heeger, *Science*, 1995, **270**, 1789–1791.

2 A. J. Heeger, *Adv. Mater.*, 2014, **26**, 10–28.

3 R. C. Haddon, A. S. Perel, R. C. Morris, T. T. M. Palstra, A. F. Hebard and R. M. Fleming, *Appl. Phys. Lett.*, 1995, **67**, 121–123.

4 A. Dodabalapur, H. E. Katz, L. Torsi and R. C. Haddon, *Science*, 1995, **269**, 1560–1562.

5 C. Wang, H. Dong, W. Hu, Y. Liu and D. Zhu, *Chem. Rev.*, 2012, **112**, 2208–2267.

6 K. Tanigaki, T. W. Ebbesen, S. Saito, J. Mizuki, J. S. Tsai, Y. Kubo and S. Kuroshima, *Nature*, 1991, **352**, 222–223.

7 A. Y. Ganin, Y. Takabayashi, P. Jeglič, D. Arčon, A. Potočnik, P. J. Baker, Y. Ohishi, M. T. McDonald, M. D. Tzirakis, A. McLennan, G. R. Darling, M. Takata, M. J. Rosseinsky and K. Prassides, *Nature*, 2010, **466**, 221–225.

8 P. W. Stephens, L. Mihaly, P. L. Lee, R. L. Whetten, S. M. Huang, R. Kaner, F. Deiderich, K. F. Holczer, *Nature*, 1991, **351**, 632–624.

9 C. Joachim, J. K. Gimzewski and H. Tang, *Phys. Rev. B*, 1998, **58**, 16407–16417.

10 R. C. Haddon, A. S. Perel, R. C. Morris, T. T. M. Palstra, A. F. Hebard and R. M. Fleming, *Appl. Phys. Lett.*, 1995, **67**, 121–123.

11 D. Bonifazi, O. Enger and F. Diederich, *Chem. Soc. Rev.*, 2007, **36**, 390–414.

12 L. Sanchez, R. Otero, J. M. Gallego, R. Miranda and N. Martin, *Chem. Rev.*, 2009, **109**, 2081–2091.

13 J. V. Barth, G. Costantini and K. Kern, *Nature*, 2005, **437**, 671–679.

14 E. I. Altman and R. J. Colton, *Surf. Sci.*, 1992, **279**, 49–67.

15 E. I. Altman and R. J. Colton, *Surf. Sci.*, 1993, **295**, 13–33

16 E. I. Altman and R. J. Colton, *Phys. Rev. B*, 1993, **48**, 18244

17 E. Mena-Osteritz and P. Bäuerle, *Adv. Mater*., 2006, **18**, 447–451.

18 J. M. MacLeod, O. Ivasenko, C. Fu, T. Taerum, F. Rosei and D. F. Perepichka, *J. Am. Chem. Soc*., 2009, **131**, 16844–16850.

19 S. Stepanow, M. Lingenfelder, A. Dmitriev, H. Spillmann, E. Delvigne, N. Lin, X. B. Deng, C. Z. Cai, J. V. Barth and K. Kern, *Nat. Mater.*, 2004, **3**, 229–233.

20 G. Pan, J. Liu, H. Zhang, L. Wan, Q. Zheng and C. Bai, *Angew. Chem. Int. Ed.*, 2003, **42**, 2747–2751.

21 J. A. Theobald, N. S. Oxtoby, M. A. Phillips, N. R. Champness and P. H. Beton, *Nature*, 2003, **424**, 1029–1031.

22 D. Bonifazi, H. Spillmann, A. Kiebele, M. de Wild, P. Seiler, F. Y. Cheng, H. J. Güntherodt, T. Jung and F. Diederich, *Angew. Chem. Int. Ed.*, 2004, **43**, 4759–4763.

23 H. L. Zhang, W. Chen, L. Chen, H. Huang, J. Yuhara and A. T. S. Wee, *Small*, 2007, **3**, 2015–2018.

24 S. Yoshimoto, E. Tsutsumi, R. Narita, Y. Murata, M. Murata, K. Fujiwara, K. Komatsu, O. Ito and K. Itaya, *J. Am. Chem. Soc.*, 2007, **129**, 4366–4376.

25 Y.-C. Yang, C.-H. Chang and Y.-L. Lee, *Chem. Mater.*, 2007, **19**, 6126–6130.

Nanoscale Accepted Manuscript

26 L. Sanchez, N. Martín and D. M. Guldi, *Angew. Chem. Int. Ed.*, 2005, **44**, 5374–5382.

27 E.-Y. Zhang and C.-R. Wang, *Curr. Opin. Colloid Interface Sci.*, 2009, **14**, 148–156.

28 F. Diederich, M and Gómez-López, *Chem. Soc. Rev.*, 1999, **28**, 263–278.

29 A. P. H. J. Schenning, P. Jonkheijm, E. Peeters and E. W. Meijer, *J. Am. Chem. Soc.*, 2001, **123**, 409–416.

30 N. Watanabe, N. Kihara, Y. Forusho, T. Takata, Y. Araki and O. Ito, *Angew. Chem. Int. Ed.*, 2003, **42**, 681–683.

31 H. Sasabe, N. Kihara, Y. Forusho, K. Mizuno, A. Ogawa and T. Takata, *Org. Lett.*, 2004, 6, 3957–960.

32 T. Haino, E. Hirai, Y. Fujiwara and K. Kashihara, Angew. Chem. Int. Ed., 2010, **49**, 7899–7903.

33 R. Otero, J. M. Gallego, A. L. V. de Parga, N. Martin and R. Miranda, *Adv. Mater.*, 2011, **23**, 5148–5176.

34 Y. S. Zhou, B. Wang, S. Q. Xiao, Y. L. Li and J. G. Hou, *Appl. Surf. Sci.*, 2006, **252**, 2119–2125.

35 M. Matsumoto, J. Inukai, S. Yoshimoto, Y. Takeyama, O. Ito and K. Itaya, *J. Phys. Chem. C*, 2007, **111**, 13297–13300.

36 C. Jehoulet, Y. S. Obeng, Y. T. Kim, F. M. Zhou and A. Bard, *J. Am. Chem. Soc.*, 1992, **114**, 4237–4247.

37 R. J. Wilson, G. Meijer, D. S. Bethune, R. D. Johnson, D. D. Chambliss, M. S. de Vries, H. E. Hunziker and H. R. Wendt, *Nature*, 1990, **348**, 621−622.

38 T. Sakurai, X.-D. Wang, Q. K. Xue, Y. Hasegawa, T. Hashizume and H. Shinohara, *Prog. Surf. Sci*., 1996, **51**, 263–408.

39 N. Katsonis, A. Marchenko and D. Fichou, *Synth. Met.*, 2003, **137**, 1453–1455.

[40] In the $R^x_y(Z)$ notation of cyclic H bonded synthons *x* and *y* represent the number of *H* bond donor and acceptor centers. Z is the total number of atoms in the ring.

41 R. Pankajavallia, C. Mallikaa, O.M. Sreedharana, M. Premilab and P. Gopalanb, *Thermochim. Acta*, 1998, **317**, 101-108.

42 C. T. Tzeng, W. S. Lo, J. Y. Yuh, R. Y. Chu and K. D. Tsuei, *Phys. Rev. B*, 2000, **61**, 2263–2272.

43 L.-L. Wang and H.-P. Cheng, *Phys. Rev. B*, 2004, **69**, 165417.

44 X. Lu, M. Grobis, K. H. Khoo, S. G. Louie and M. F. Crommie, *Phys. Rev. B*, 2004, **70**, 115418.

45 M. Hinterstain, X. Torrelles, R. Felici, J. Rius, M. Huang, S. Fabris, H. Fuess and M. Pedio, *Phys. Rev. B*, 2008, **77**, 153412.

46 M. A. Mezour, O. Voznyy, E. H. Sargent, R. B. Lennox and D. F. Perepichka, *submitted*.

47 W. Azzam, A. Bashir, P. Ulrich Biedermann and M. Rohwerder, *Langmuir*, 2012, **28**, 10192–10208.

[48] Occasionally, clusters $C_{61}(CO_2H)_2$ were also observed to form on BT SAM in the same conditions; however, these appeared to be less stable. No stable (at STM time scale) cluster of C61(CO2H)2 were observed at HOPG/phenyloctane interface.

49 A. Hirsch and O. Vostrowsky, *Eur. J. Org. Chem*., 2001, 829–848.

50 Z. Li. B. Han, L. J. B. Wan and T. Wandlowski, *Langmuir*, 2005, **21**, 6915–6928.

51 A. Hirsch, I. Lamparth and H. R. Karfunkel, *Angew. Chem. Int. Ed.*, 1994, **33**, 437–438.

52 A. Hirsch, I. Lamparth, T. Grösser and H. R. Karfunkel, *J. Am. Chem. Soc.*, 1994, **116**, 9385–9386.

Nanoscale Accepted Manuscript

53 I. Lamparth, C. Maichle-Mössmer and A. Hirsch, *Angew. Chem. Int. Ed.*, 1995, **34**, 1607–1609.

Nanoscale Accepted Manuscript